AGU PUBLICATIONS

Journal of Advances in Modeling Earth Systems

RESEARCH ARTICLE

10.1002/2014MS000397

An empirical model relating U.S. monthly hail occurrence to large-scale meteorological environment

John T. Allen[1], Michael K. Tippett[2,3], and Adam H. Sobel[2,4]

[1]IRI, Earth Institute, Columbia University, Palisades, New York, USA, [2]Department of Applied Physics and Applied Mathematics, Columbia University, New York, New York, USA, [3]Center of Excellence for Climate Change Research, Department of Meteorology, King Abdulaziz University, Jeddah, Saudi Arabia, [4]Department of Earth and Environmental Sciences, Columbia University, New York, New York, USA

Key Points:
- Develops an empirical model to describe hail occurrence over the U.S.
- Index is capable of capturing the interannual and seasonal variability of hail
- Discusses the limitations of existing hail climatology from observations

Correspondence to:
J. T. Allen,
JohnTerrAllen@gmail.com

Citation:
Allen, J. T., M. K. Tippett, and A. H. Sobel (2015), An empirical model relating U.S. monthly hail occurrence to large-scale meteorological environment, *J. Adv. Model. Earth Syst.*, *7*, 226–243, doi:10.1002/2014MS000397.

Received 16 OCT 2014
Accepted 18 DEC 2014
Accepted article online 9 JAN 2015
Published online 20 FEB 2015

Abstract An empirical model relating monthly hail occurrence to the large-scale environment has been developed and tested for the United States (U.S.). Monthly hail occurrence for each 1°×1° grid box is defined as the number of hail events that occur there during a month; a hail event consists of a 3 h period with at least one report of hail larger than 1 in. The model is derived using climatological annual cycle data only. Environmental variables are taken from the North American Regional Reanalysis (NARR; 1979–2012). The model includes four environmental variables convective precipitation, convective available potential energy, storm relative helicity, and mean surface to 90 hPa specific humidity. The model differs in its choice of variables and their relative weighting from existing severe weather indices. The model realistically matches the annual cycle of hail occurrence both regionally and for the contiguous U.S. (CONUS). The modeled spatial distribution is also consistent with the observed hail climatology. However, the westward shift of maximum hail frequency during the summer months is delayed in the model relative to observations, and the model has a lower frequency of hail just east of the Rocky Mountains compared to observations. Year-to-year variability provides an independent test of the model. On monthly and annual time scales, the model reproduces observed hail frequencies. Overall model trends are small compared to observed changes, suggesting that further analysis is necessary to differentiate between physical and nonphysical trends. The empirical hail model provides a new tool for exploration of connections between large-scale climate and severe weather.

1. Introduction

Hail is responsible for significant damage to agricultural resources, vehicles, and buildings. While hail damage in the United States (U.S.) is less extreme than that due to tornadoes, hail affects larger areas on a more regular basis, resulting in U.S. annual losses of near 1 billion U.S. dollars of the estimated 1.6 billion annual total for severe thunderstorms [*Changnon*, 1999, 2008; *Munich*, 2013]. The U.S. National Climatic Data Center's (NCDC) Storm Data observational hail record is the most comprehensive publicly available data set. However, the Storm Data hail reports have a number of deficiencies [*Schaefer and Edwards*, 1999; *Doswell et al*., 2005; *Doswell*, 2007]. For example, only maximum hail size is reported, and that value may be quantized or distorted by association to reference objects (e.g., golf balls). Recent high-resolution hail observations from field campaigns [e.g., *Ortega et al*., 2009; *Blair et al*., 2014] suggest that larger hail sizes are more common than would be expected from Storm Data hail reports. Another characteristic of the Storm Data hail reports are positive trends in the frequency of hail in excess of 2 in. in diameter (hereafter giant hail), especially over the southeast of the U.S. [*Schaefer et al*., 2004]. These trends skew heavily toward areas of higher population density, and where National Weather Service forecast offices actively seek out hail reports for the warning verification process [*Hales*, 1993; *Wyatt and Witt*, 1997; *Davis and LaDue*, 2004; *Schaefer et al*., 2004; *Trapp et al*., 2006; *Cintineo et al*., 2012]. These factors limit the direct analysis of temporal and spatial variability in the Storm Data hail report data for climate studies.

An alternative approach is to consider the environments that are favorable to hail occurrence [*Brooks et al*., 2003; *Brooks*, 2009]. The majority of hailstones 1 in. or larger (hereafter large hailstones) are associated with organized thunderstorms [*Kelly et al*., 1985], and nearly all instances of giant hail are associated with supercell thunderstorms, though such stones may only be a small fraction of the total hail from a storm

This is an open access article under the terms of the Creative Commons Attribution-NonCommercial-NoDerivs License, which permits use and distribution in any medium, provided the original work is properly cited, the use is non-commercial and no modifications or adaptations are made.

© 2015. The Authors.

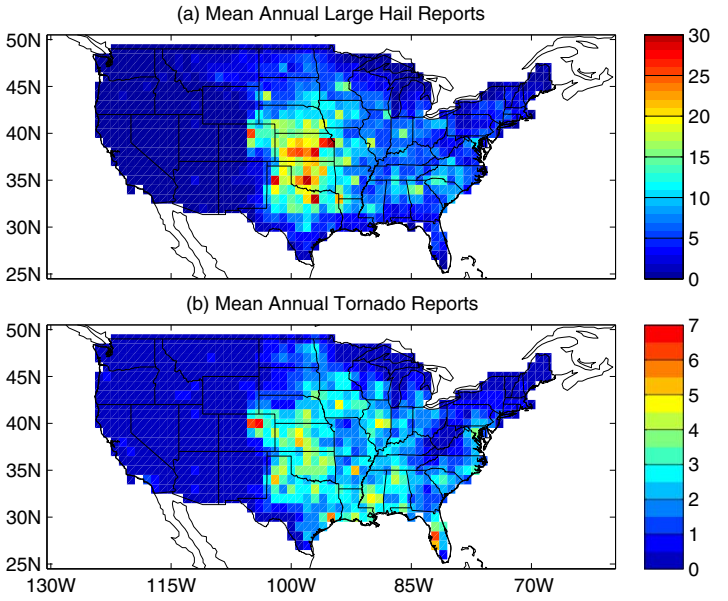

Figure 1. (a) Annual mean number of gridded (1°×1°) reports of hail equal to or greater than 1 in. 1979–2012, and (b) annual mean number of gridded (1°×1°) reports of tornadoes greater than F0 intensity for the same period.

[*Changnon et al*., 2009]. Hail occurrence has previously been related to the thermodynamic potential of the severe thunderstorm environment [*Stumpf et al*., 2004; *Giaiotti et al*., 2003; *Groenemeijer and Van Delden*, 2007; *Kunz et al*., 2009; *Grams et al*., 2012; *Thompson et al*., 2012], particularly the steepness of midlevel lapse rates, suspension of ice nuclei in the optimum hail growth region, as well as moisture availability. While thermodynamic sources of energy are essential to promote the strong updrafts that support hail, shear enhancement of the vertical pressure gradient provides another important contribution [*Edwards and Thompson*, 1998; *Doswell and Markowski*, 2004; *Jewell and Brimelow*, 2009; *Grams et al*., 2012; *Manzato*, 2012]. The interaction between thermodynamic potential and vertical wind shear is quantified, for example, in the Significant Hail Parameter (SHIP; details of the formula for SHIP can be found at http://www.spc.noaa.gov/exper/mesoanalysis/help/help_sigh.html). SHIP is a function of convective available potential energy (CAPE), the mixing ratio of a parcel, environmental midlevel lapse rate, 500 hPa temperature, and 0–6 km vertical wind shear (S06) and is a measure of the favorability of environmental conditions for giant hail. In comparison, the significant severe parameter (SSP) of *Brooks et al*. [2003] attempts to capture the occurrence of giant hail as well as damaging winds and strong tornadoes based on the weighted product of CAPE and S06. These severe weather indices are widely applied to sounding or subdaily model data and used in short-range weather forecasting.

The greater dependence of SHIP on the thermodynamics of the profile compared to the SSP illustrates that complex interactions on the microphysical scale, moisture loading, as well as the structure of the vertical temperature profile can influence the potential for large hail in ways that are different than other forms of severe weather. Consequently, measures of the favorability of the environment for tornadoes [*Tippett et al*., 2012, 2014] and significant severe thunderstorms [*Brooks et al*., 2003; *Gensini and Ashley*, 2011] may be suboptimal for estimating hail occurrence. As illustrated by *Brooks* [2013], tornadoes, hail, and damaging wind favor different parts of the environmental phase space of thermodynamic and kinematic conditions.

Spatial maps over the contiguous U.S. (CONUS) of the average number of tornado and large hail reports per year for the period 1979–2012 are shown in Figure 1. Relative to the tornado climatology, hail is found further west, reflecting the occurrence of hail-producing storms along the dryline in the high plains into the Texas panhandle. Hail is also less frequently found over the southeast of the CONUS where lapse rates are generally lower [*Cintineo et al*., 2012]. In addition, hail is reported more often in the U.S. than tornadoes, with an average of 4191 large hail events per year compared to 1007 tornado reports per year for the period 1979–2012. While most assessments of hail risk for the United States have relied mainly on databases of hail reports [*Doswell et al*., 2005; *Changnon et al*., 2009], more recently remote sensing approaches based on radar reflectivity or satellite cloud top temperatures have been used [*Cintineo et al*., 2012; *Cecil and Blankenship*, 2012]. However, changing technology in radar output for the U.S. and satellites limit both of these methods to about the last decade. The satellite approach, while global in coverage, tends to overestimate hail occurrence over the tropics where large hail is rarely observed [*Knight and Knight*, 2001; *Cecil and Blankenship*, 2012]. The radar-derived climatology in contrast is limited by spatial extent to available

© 2015. The Authors.

radar sites, temporal period due to changing technology, and shows poor size discrimination for hail larger than 4.9 cm [*Cintineo et al*., 2012].

Attempts to relate hail occurrence to the large-scale environment have generally focused on small regions utilizing synoptic composites [e.g., *Cao*, 2008; *Kapsch et al*., 2012] or station proximity analyses [e.g., *Edwards and Thompson*, 1998]. More recently, empirical hail models have been applied to estimate frequency or size from the environmental conditions [e.g., *Jewell and Brimelow*, 2009; *Sanderson et al*., 2014]. A small number of studies have investigated both univariate and multivariate, as well as linear and nonlinear discriminants for hail [e.g., *Manzato*, 2012; *Eccel et al*., 2012; *Manzato*, 2013]. These have mainly focused on atmospheric variables using limited data samples over small regions, or covariates such as used by *Brooks et al*. [2003].

The aim of this study is to construct a model to predict hail occurrence from the large-scale environmental conditions. While our use of data over a large region (CONUS) and long period (34 years) is distinguishing, the main difference of the work here is our choice to use monthly averages, and to a lesser extent, the choice to use spatial scales on the order of 100 km. The motivation for this choice is our interest in the modulation of severe weather occurrence by climate variability on both seasonal and longer time scales. Therefore, the specific goal here is to develop a model to predict monthly hail occurrence from monthly averaged environmental variables. The obvious difficulty with this goal is that hail occurrence is mostly directly related to the Instantaneous local values of the environment, not monthly averages.

We develop the hail occurrence model using only annual cycle data. In doing so, we are testing the hypothesis that the monthly hail occurrence climatology is related to the climatological distribution of monthly mean environments. Since we develop the model in a regression framework, we can test this hypothesis by testing the significance of regression coefficients, as well as by evaluating the degree to which the model is able to reproduce spatial and temporal features of the hail climatology. Having developed the model using only annual cycle data, the ability of the model to match observed interannual variability is an independent validation of the model and a test of the hypothesis that variations in monthly environments are reflected in hail occurrence.

This paper is structured as follows: section 2 describes the hail observations and the North American Regional Reanalysis (NARR) used for environmental data. Section 3 details the development of the statistical model relating hail occurrence to the large-scale environment and compares it to other potential models. Sections 4 and 5 explore the seasonal, interannual, and spatial characteristics of the model on both a CONUS-wide and regional basis. Finally, in section 6, the limitations of the model and our approach are discussed, and the future potential applications of this index are outlined.

2. Data

2.1. NCDC Storm Data: Hail

A $1^\circ \times 1^\circ$ U.S.-wide gridded data set of monthly hail occurrence was constructed based on the NCDC storm data for the period 1979–2012 [*Schaefer and Edwards*, 1999]. We define the monthly hail occurrence for each grid box and month as the number of three-hourly periods (0Z–3Z, 3Z–6Z, etc.) with at least one report of 1 in. or larger hail. We chose this definition of a hail event, with its binning in time and space, to reduce the influence of nonmeteorological factors such as population and road distributions. For example, Figure 2a shows that reports of large hail near Amarillo, Texas, have distinct small-scale spatial structure that is more likely related to road networks and population than to meteorological variations. The clear imprint of the road network on hail reports suggests that simple corrections for report biases using population density alone are likely to be of limited effectiveness. Despite the spatial binning, a substantial east-to-west decrease in monthly hail occurrence remains (Figure 2b), coinciding with the dropoff in population and road network density. The 1 in. threshold also serves to remove some sampling and observer issues that result from quantized biases toward the minimum threshold which was 0.75 in. for the period 1979–2010 before its elevation to 1 in. in 2010 [*Schaefer et al*., 2004]. Finally, only the monthly annual cycle of hail occurrence (a single value for each of the 12 calendar months at each location) is used to develop the model, thereby removing trends from the model development procedure.

2.2. North American Regional Reanalysis

The North American Regional Reanalysis (NARR) [*Mesinger et al*., 2006] provides environmental data. The reanalysis has a horizontal resolution of 32 km. For this application, the data were bilinearly interpolated to

© 2015. The Authors.

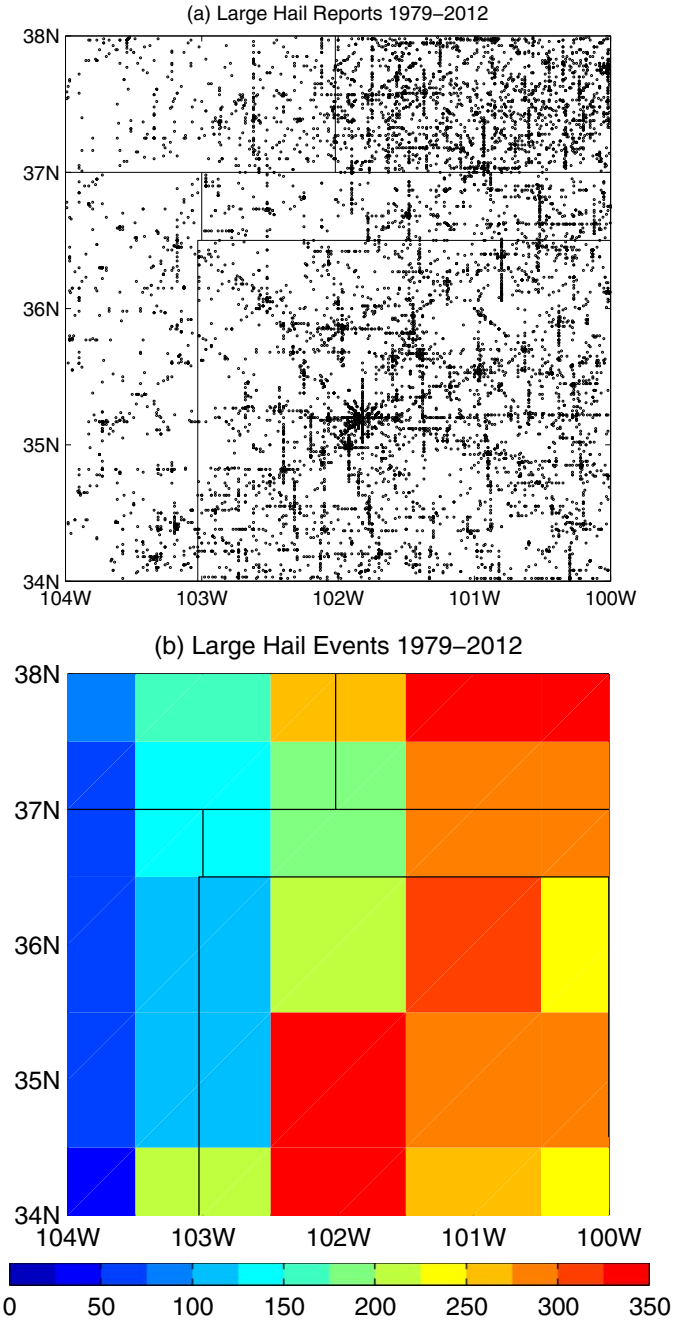

Figure 2. (a) Point reports of hail over the period 1979–2012 for the Texas panhandle and surrounding areas bounded by 34°N–38°N and 104°W–100°W from NCDC hail observations, and (b) total number of gridded (1°×1°) three-hourly hail events (≥1 in.) for the same period and domain.

the same 1°×1° grid over the CONUS (25°N–50°N, 130°W–60°W) used for the hail observations. Twenty monthly mean parameters were chosen for potential inclusion in the model. These included thermodynamic and kinematic quantities, parameters commonly used for hail detection in an operational setting, as well as other parameters potentially related to the seasonal cycle (Table 1). We take the logarithm of some of the variables, motivated by the findings of *Brooks et al.* [2003] and *Brooks* [2013]. In addition, parameters relating to observational characteristics including 1°×1° gridded elevation and population were also considered.

NARR wind fields and calculated measures of vertical wind shear have been shown to be realistic, particularly outside of the planetary boundary layer where subgrid-scale influences become more important [*Gensini et al.*, 2014]. NARR thermodynamic quantities in contrast have been shown to have several limitations. The deficiencies in NARR thermodynamics partly relate to the activation of shallow convection within the Eta model convection scheme used to produce the reanalysis, which results in large amounts of drying between 900 and 700 hPa and strongly influences the development of both instability and convective inhibition [*Baldwin et al.*, 2002; *Gensini et al.*, 2014]. However, for parameters such as convective precipitation, NARR could be potentially advantageous, since the assimilation of precipitation as latent heat profiles can assist in damping activity in the model's convective scheme [*Mesinger et al.*, 2006; *Bukovsky and Karoly*, 2007].

3. Model Development

Several approaches have been used previously to fit statistical relationships between observed severe weather and environment [e.g., *Brooks et al.*, 2003; *Eccel et al.*, 2012; *Manzato*, 2013; *Elsner and Widen*, 2014]. Here we use Poisson regression, which assumes a log linear relationship between the environmental

© 2015. The Authors.

Table 1. List of Parameters Chosen for Relationship Selection[a]

Input Parameters	Abbreviation	Units
0–3 km storm relative helicity	*SRH*	$m^2\ s^{-2}$
500 hPa temperature	*T500*	K
700–500 hPa lapse rate	LAPSE	$^\circ C\ km^{-1}$
180 hPa MLCAPE	*MLCAPE*	$J\ kg^{-1}$
180 hPa MLCIN	*MLCIN*	$J\ kg^{-1}$
Convective precipitation	*cPrcp*	$kg\ m^{-2}$
Surface-based CAPE	*SBCAPE*	$J\ kg^{-1}$
Surface-based CIN	*SBCIN*	$J\ kg^{-1}$
Geop. height of zero isotherm	*FZL*	m
Most unstable lifted index	*LI*	K
0–1 km bulk wind shear	S01	$m\ s^{-1}$
0–6 km bulk wind shear	S06	$m\ s^{-1}$
0–8 km bulk wind shear	S08	$m\ s^{-1}$
6 km to tropopause wind shear	S6TP	$m\ s^{-1}$
Relative height of LCL	rLCL	hPa
Mixed-layer LCL	MLLCL	hPa
Surface equivalent pot. temp.	ThetaE	K
Mean RH surf. to zero isotherm	MeanRHZero	%
Mean 2 m to 90 hPa specific humidity	Q_{mean}	$g\ kg^{-1}$
Soil moisture in 1 m layer	*SoilM01*	$kg\ m^{-2}$

[a]Italics denote modeled parameters, while underlining indicates the logarithm of a parameter was used. LAPSE, S01, S06, S08, and S6TP were all calculated using the respective temperature or wind fields at given layers. LCL height was calculated following the approach of *Craven et al.* [2002] for a mixed-layer parcel and scaled using relative height from ground in hPa. Moisture means MeanRHZero and Q_{mean} were calculated using relative and specific humidity from the surface (2 m) to the 0° isotherm and 90 hPa above the surface, respectively.

parameters and the number of hail events. The same approach has previously been applied to tropical cyclones [*Tippett et al.*, 2011] and tornadoes [*Tippett et al.*, 2012]. An offset term accounts for the different area of each grid box and the number of years in the climatology. The Poisson distribution assumption is relevant in the maximum-likelihood estimation of the regression coefficients, and to the extent that this distributional form is not appropriate, there is potential for more accurate estimates of the regression coefficients. We do not use the statistics or percentiles of the Poisson distribution and avoid any assumptions on the equality of conditional mean and variance. Overdispersion results if the variance of the data exceeds the conditional mean [*Elsner and Widen*, 2014]. To address the sensitivity of the results here to choice of distribution, negative binomial regression was also tested. The negative binomial regression results in similar regression coefficient estimates, but increased sum-squared error.

One of the dangers of fitting any regression is overfitting, where an excessive number of predictors results in poor performance in independent data. The regression fitting procedure here uses the climatological annual cycle of monthly hail occurrence (12 values) at each U.S. grid point (860 grid points) for a total of 10,320 samples with the corresponding climatological annual cycle values of the parameters listed in Table 1; the regression coefficients do not depend on location or month. The risk of overfitting is reduced since the (nominal) sample size greatly exceeds the number of predictors. Nonetheless, a model with as few predictors as possible is desirable. We use cross validation to measure performance on independent data, and the number of parameters is increased until the addition of further parameters results in minimal cross-validated gain. The deviance is a measure of the goodness of fit and for a Poisson regression is calculated as:

$$\text{Deviance} = 2\sum_{i=1}^{n} y_i\ \ln\left(y_i/\mu_i\right) - \left(y_i - \mu_i\right), \tag{1}$$

where y is the number of hail events, n is the number of observations, and μ is the fitted hail model. For the fitting procedure, the second term of deviance reduces to zero by design as the model captures the average. For the out-of-sample calculations in the cross-validation and interannual data, this term is nonzero and thus contributes to the deviance. The mean and standard deviation of the deviance is computed using 10 iterations of 10-fold cross validation. The observations used to compute the cross-validated deviance are separate from those used to fit the index. Figure 3 shows that after four predictors are included in the model, additional parameters do not substantially improve the fit. We obtain the coefficients and parameters for the hail model as:

$$\begin{aligned}\mu_{\text{Hail}} = \exp\big[&-10.18 + 0.97\log\left(\text{cPrcp}\right) + 1.13\log\left(\text{SRH}\right)\\ &+ 1.00\log\left(\text{MLCAPE}\right) - 0.31\text{Q}_{mean} + \log\left(\Delta x\,\Delta y\,T\cos\phi\right)\big],\end{aligned} \tag{2}$$

where the final term is the offset, with ϕ as the latitude, Δx and Δy are the longitude and latitude spacings in degrees, respectively, and T is the number of years. Table 2 gives the uncertainty (plus/minus two standard deviations) of the regression coefficients estimates as calculated during the cross validation. The

© 2015. The Authors.

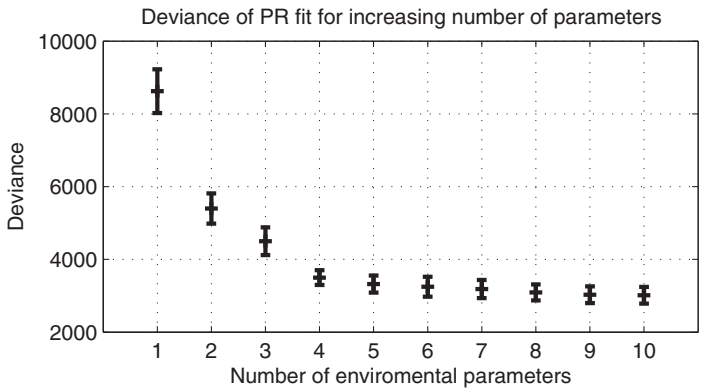

Figure 3. Deviance of model as function of the number of environmental parameters. The central point and error bars indicate the mean and standard deviation of deviance calculated using 10 iterations of 10-fold cross validation.

coefficients are highly significant in all cases, supporting our hypothesis that the monthly hail occurrence climatology is related to the climatological distribution of monthly mean environments. The tornado index by comparison is [*Tippett et al*., 2012, 2014]:

$$\mu_{\text{Tornado}} = \exp\left[-10.59 + 1.36\log(\text{cPrcp}) + 1.89\log(\text{SRH}) + \log(\Delta x\,\Delta y\,T\cos\phi)\right]. \quad (3)$$

The hail model is substantially different from the tornado index, reflecting the different spatial distribution and environmental conditions that precede the respective thunderstorm phenomena. Figure 3 indicates that the deviance from the hail data is reduced significantly by addition of the third and fourth parameters. This was not the case for the tornado data, where using more than two parameters did not improve the index fit. The index for tornadoes, in comparison to the four-parameter hail model, is more sensitive to variations in SRH. This difference is expected, as tornadoes are more reliant than hail on the presence of low-level environmental wind shear [*Brooks et al*., 2003]. The importance of cPrcp is also reduced in the four-parameter index hail model relative to the tornado index. Comparing the hail index to the potential three-parameter fit, the dependence on SRH decreases by almost a half (Table 2). Compensating for this change, the dependence on MLCAPE doubles, while the coefficient for cPrcp also increases by a third. As we introduce addition components to the model, the fitting procedure varies the respective coefficients to maximize the likelihood. The colinearity of the respective components means that introducing parameters with common characteristics (moisture) results in the coefficients being varied to maximize the fit. The introduction of the negative sign fourth parameter Q_{mean} allows each of the other coefficients to be adjusted upward, thereby improving the fit. As shown by the changes to the deviance (Figure 3), there is little additional variance explained by the introduction of additional parameters, and thus any adjustment to the coefficients only results in a trivial improvement in model performance.

The log linear assumption was checked by performing a bootstrapped fitting procedure between the tenth and ninetieth percentiles of the values for each environment variable and ensuring it displayed a logarithmic relationship as in *Tippett et al*. [2014]. This assumption was found to be appropriate except for small values of Q_{mean}, over which range the regression coefficients were positive (not shown) in contrast to the negative value in the index. These small values of Q_{mean} only occur for a few grid points in the northern CONUS during January, February, and March, where moisture limitation may be important.

To examine the relative contributions of the variables in the model, we show maps in Figure 4 of the annual number of hail events as the number of variables in the model increases from one to four. cPrcp is the first parameter selected by the forward selection procedure, which is unsurprising given its appearance in the tornado index and its prior utility for characterizing convective initiation [*Trapp et al*., 2009]. Physically, cPrcp is a consequence of both convective initiation by the model's convective parameterization scheme and the

Table 2. Hail Model Coefficients for Increasing Number of Parameters and Plus/Minus Their Two Standard Error Uncertainty as Estimated in the Cross-Validation Procedure

Coefficients	Intercept	cPrcp	SRH	MLCAPE	Q_{mean}
One parameter	-2.33 ± 0.025	1.10 ± 0.014			
Two parameter	-10.07 ± 0.133	1.48 ± 0.030	1.86 ± 0.015		
Three parameter	-14.88 ± 0.168	0.72 ± 0.027	2.03 ± 0.013	0.51 ± 0.023	
Four parameter	-10.33 ± 0.177	0.99 ± 0.030	1.14 ± 0.016	1.00 ± 0.023	-0.31 ± 0.007
Tornado	-10.59 ± 0.179	1.36 ± 0.041	1.89 ± 0.019		

© 2015. The Authors.

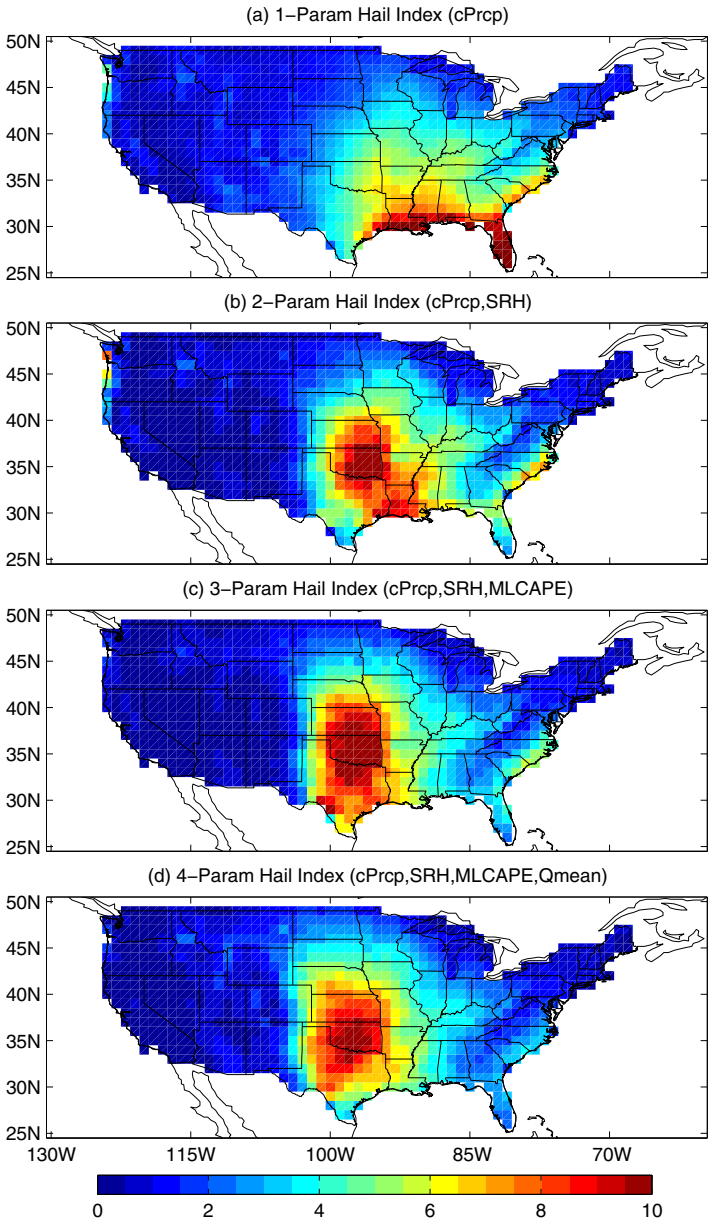

Figure 4. Optimal deviance fitted Poisson regression indices for large hail events with increasing number of environmental parameters for the period 1979–2012. (a) One parameter index (cPrcp), (b) two parameter index (cPrcp, SRH), (c) three parameter index (cPrcp, SRH, MLCAPE), and (d) four parameter index (cPrcp, SRH, MLCAPE, Q_{mean}). Units are mean annual number of three-hourly periods with hail events greater than 1 in.

thermodynamic instability present. Precipitation then occurs until the instability is resolved by the parameterization scheme, with the magnitude of the resultant convective rainfall constrained by assimilation of precipitation data as latent heat profiles in the NARR reanalysis. However, the hail model with cPrcp alone does not produce a useful distribution for hail occurrence, with peak values confined to the Gulf of Mexico coast and close to the source of moisture (Figure 4a). The two-parameter model, like that for tornadoes, includes SRH, although with stronger weighting and is shifted over the plains relative to the tornado climatology but with similar coefficients (Table 2 and Figure 4c). Again, the inclusion of SRH is physically reasonable, reflecting the potential for organized thunderstorms and rotating updrafts characteristic of supercells, the producers of a significant fraction of large hail. Adding a third parameter results in inclusion of a direct measure of the potential updraft strength, MLCAPE. Unlike cPrcp, which describes a model response to available energy and varies depending on the atmospheric moisture content and other factors, MLCAPE describes the potential energy available to updrafts over a given month in the climatological cycle. Since this parameter was calculated with a mixed-layer parcel depth of 180 hPa, the deep parcel is also likely a reflection of the convective inhibition present within the atmosphere, perhaps explaining the westward shift of the climatological maximum in the index in addition to the expected thermodynamic relationship. The three-parameter model produces a greater hail frequency over the southern half of Texas compared to observations, but is improved compared to the two-parameter model. We suspect that this is a result of convective inhibition being handled poorly by many reanalysis products including NARR as seen for combinations of CAPE and S06 in this area [*Brooks et al.*, 2003; *Gensini and Ashley*, 2011]. The deviance is further reduced by the addition of a fourth parameter, Q_{mean} (Figure 4d). On a diurnal scale, this parameter is representative of moisture in the boundary layer, and the potential for loading of precipitable water within the updrafts of storms. However, these characteristics are unlikely

© 2015. The Authors.

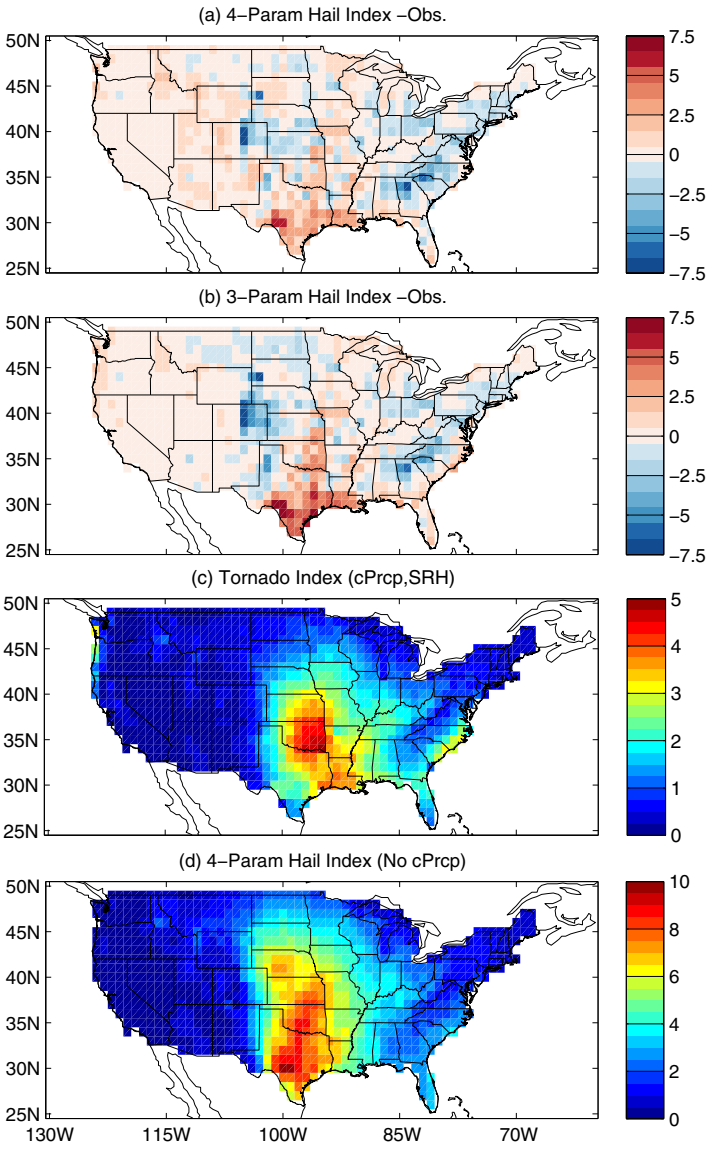

Figure 5. (a) Difference between the mean annual number of three-hourly periods with hail events for the four-parameter hail model and observed large hail events 1979–2012. (b) As for Figure 5a, except difference between mean annual number of the three-parameter hail index events and observed large hail events. (c) Mean annual number of three-hourly periods with tornado events from the tornado index calculated using equation (3) for the same period. (d) Mean annual number of large hail events of the "next best" index without cPrcp included.

to be represented in monthly averages. The spatial distribution of the four-parameter model produces a more accurate representation of hail events in the Texas panhandle, eastern New Mexico, and eastern Colorado.

These coefficient changes, together with the addition of Q_{mean}, improve the spatial distribution over the problematic southern Texas and coastal areas when compared to the three-parameter hail model (Figures 5a and 5b). Q_{mean} however does not improve errors near the Front Range of the Rocky Mountains where additional moisture should be favorable to the development of hail, prompting further scrutiny. The correlation of Q_{mean} with the hail model and with the monthly hail occurrence data is positive and significant, which is physically sensible. It is therefore surprising that the coefficient of Q_{mean} in the index is negative (Table 2). This behavior can be understood by noting that Q_{mean} is well correlated with MLCAPE and cPrcp, implying that the predictors exhibit colinearity. Thus, the sign of the coefficient of Q_{mean} must take into account the relation of Q_{mean} with hail occurrence and as well as its relation with the other predictors. Here there is a negative relation between Q_{mean} and the variability unexplained by the first three predictors, and this relation results in a negative coefficient for Q_{mean} in the optimum four-parameter fit.

Two other potential indices are presented for comparison (Figures 5c and 5d). The first is the tornado index [*Tippett et al.*, 2012, 2014]. This comparison illustrates the novelty of the hail model, showing the clear differences between hail and tornado environmental relationships. While the tornado index is characterized by the double-lobe structure of the so-called Tornado and Dixie alleys, hail occurrence is more confined to the central Great Plains. This presumably reflects the greater instability and steep midlevel lapse rates in this region, downstream of the high terrain, whereas by the time such air has moved over the east, it has typically been mixed by repeated days of convection, reducing these lapse rates and instability [*Cintineo et al.*, 2012]. We also compare the best four-parameter model to a version that does not include convective

© 2015. The Authors.

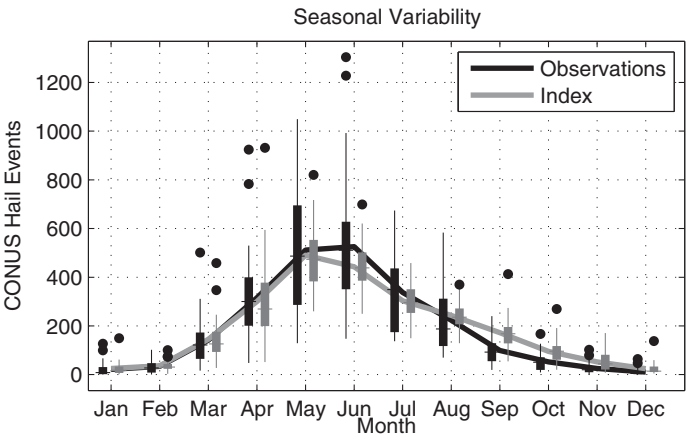

Figure 6. Seasonal variability of the hail model for total monthly hail events over the CONUS as compared to observed hail events 1979–2012. Lines are mean index (gray) and observations (black) seasonal cycle, and whiskers reflect 2.7σ of the distribution (99.3%). Dots show outlying years, which are outside the 2.7σ range.

precipitation as one of the constituent parameters (Figure 5d). When ranked by minimized deviance, this corresponds to the tenth best four-parameter model. The moisture quantity Q_{mean} is found in all 10 of these indices, along with a range of shear and CAPE representations. The model index with no cPrcp includes: MLCAPE, S06, the relative height of the lifted condensation level (rLCL), and Q_{mean}. However, like many of the CAPE-shear product indices that have been applied for six-hourly data [e.g., *Brooks et al.*, 2003; *Gensini and Ashley*, 2011], this model suffers from overly high values in the southern parts of Texas where climatological CAPE is high (thereby generating high model values), but convection is rarely initiated. Including the NARR cPrcp in our model reduces this problem, though does not remove it entirely (Figure 5a).

4. Model Climatology

4.1. Annual Cycle

The model seasonal cycle is similar to that of observations, with lower year-to-year variability and some deficiencies in the mean of the seasonal cycle (Figure 6). The main difference is a small underestimation of the occurrence of hail in the peak months of May to July, and a small overestimation for the autumnal months September to November. These biases in the mean reflect two limitations of the model; in the western high plains of Colorado, the occurrence of hail over this area is underestimated by the model. A potential explanation is the reduced moisture in the NARR reanalysis compared to observations over Colorado which impacts the values of Q_{mean}, cPrcp, and MLCAPE [*Gensini et al.*, 2014]. The second problem arises over the southeast of the continent, where the model is also biased downward. The extent to which this is a real bias as compared to an observational flaw arising from the verification process has been questioned [*Cintineo et al.*, 2012]. The variability of the climatologically fitted model applied to interannually varying environment is somewhat smaller than observed for April, May, and June, although a large portion of the observations falls within the expected range. While the model does have limitations in its handling of the variability, it shows a capability to simulate the extreme outliers of the climatology outside the reduced variability (e.g., the outlying value in April).

Moving from continental scale to regional analysis, the model performs well in estimating the timing of the seasonal peak for all of the nine NOAA climate regions [*Karl and Koss*, 1984], except over the northwest where there are relatively few hail reports (Figure 7). Three different behaviors can be seen in the difference between the model and observations over the respective regions: central plains (south, central, and plains), east (southeast and northeast), and west (upper midwest and southwest). In the central plains, both peak magnitude and the timing of the seasonal cycle are well replicated (Figures 7a, 7d, and 7f). Given that a large fraction of CONUS hail occurrence is found in these regions, it is important that the model captures the seasonal cycle well, though the spread of variability of the model is reduced for both the Central and Plains regions. Despite this decreased spread in interannual variability, we will see later that interannual correlations of frequency for these regions on a monthly scale show appreciable skill during the peak months (Table 3).

Over the east of the CONUS, both the temporal structure and the summer peak of the seasonal cycle is replicated. However, the magnitude of the model is much lower than the observed frequencies (Figures 7b

© 2015. The Authors.

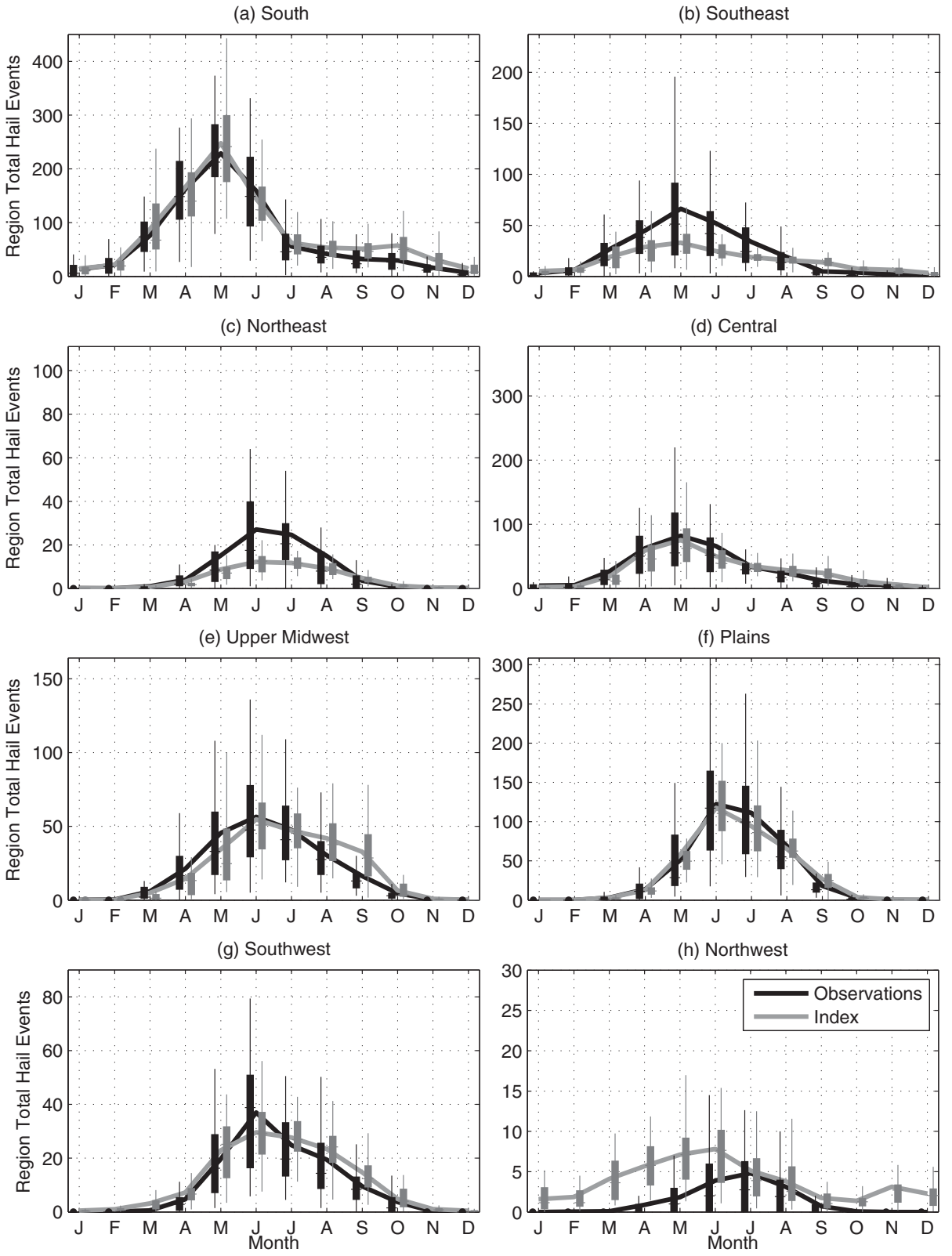

Figure 7. As for Figure 6, except seasonal cycle of the index and observed hail events over the NOAA climate regions for (a) south, (b) southeast, (c) northeast, (d) central, (e) upper midwest, (f) plains, (g) southwest, and (h) northwest. No outliers are shown.

© 2015. The Authors.

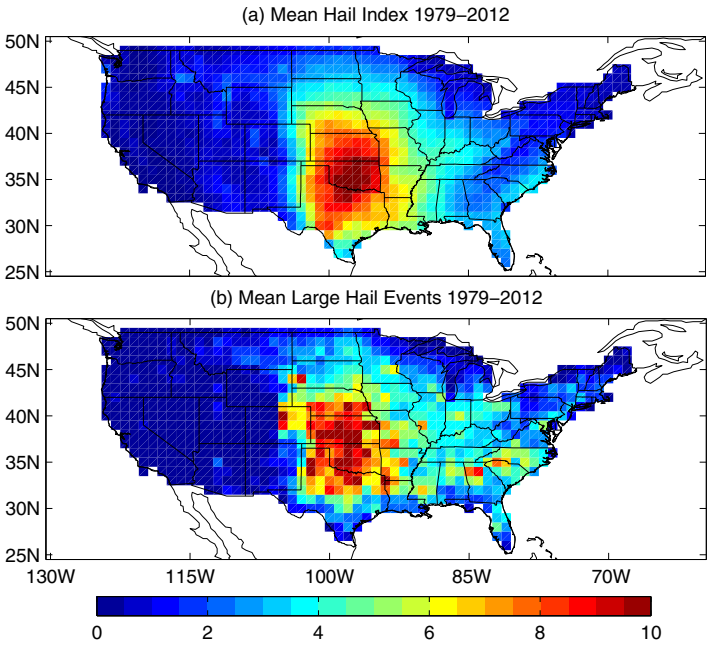

Figure 8. (a) Mean annual number of three-hourly periods with large hail events as predicted by the four parameter index 1979–2012. (b) As for Figure 8a, except the mean annual occurrence of observed large hail events.

and 7c). These underestimates are potentially related to the buoyancy-driven environments in which these storms occur, or possible biases in the reporting arising from warning verification policy [*Cintineo et al.*, 2012]. Despite these deficiencies, we will see later that significant correlations are found for all but October and December in the northeast, with the highest values during spring and the early summer (Table 4). In both the upper midwest and southwest (Figures 7e and 7g), the model simulates the peak, but does not identify the decreasing frequency of hail in the late summer and early fall. As we show later, this deficiency is reflected in poor interannual correlations between observations and the model for all months barring October in these regions. Combining both the second and third characteristics reveals that the biases in the CONUS mean annual frequency arise from regions outside of the peak climatological frequency in the center of the CONUS and suggest that regional examination of appropriate fits may be necessary to form a more precise climatology.

4.2. Annual Climatology

Despite the binning procedures used, the hail events climatology show what are potentially biases toward urban centers and frequently traversed road networks as described in section 2. The highest mean annual frequencies are found through northern Texas through Oklahoma and Kansas into southern Nebraska, with peak values between 10 and 11 hail events per year (Figure 8b). A northwestward extension occurs along the margins of the high terrain, reflecting the high frequency of hail at this altitude, while extension east is through the Missouri, Mississippi, and Ohio valleys in one belt, and a second south of the Ozark Plateau and the Appalachian mountains through the south to the Carolinas. In contrast, the maximum in the model climatology is more confined to the plains, extending from the Rio Grande valley on the Mexican border northward into southern Nebraska (Figure 8a). The spatial peak is found over northwestern and central Texas, extending through central Oklahoma and into southern Kansas, east as far as the Arkansas border and west to New Mexico. Despite the systematic bias in frequency when compared to the observed climatological frequency of hail events (Figure 5), the model has an RMSE of 1.27 hail events annually, corresponding to less than 15% of the peak magnitude of 10 events and a pattern congruence (the uncentered pattern correlation of two gridded spatial maps as described by *Wilks* [2006]) of 0.93. While significant spatial biases compared to observations are found for the western parts of the plains (including eastern Colorado, northwestern Texas, and eastern New Mexico), these differences are potentially related to the relatively sparse population in these areas (Figure 2b) [*Changnon et al.*, 2009], rather than indicating that environments favorable to hail events do not occur in these areas. Gridded population and elevation were considered for their predictive capabilities in the model for this reason, but neither were selected owing to the probably complexity of the relationship.

Peak frequencies in the model have similar magnitudes to the mean annual observational values, suggesting that this characteristic is well captured (Figure 8a). The northern extension along the Ohio valley to the east is present in the model climatology, but is displaced slightly southward. However, the model does not represent the climatological frequency over the southeast. The origins of large hail in this area may be

© 2015. The Authors.

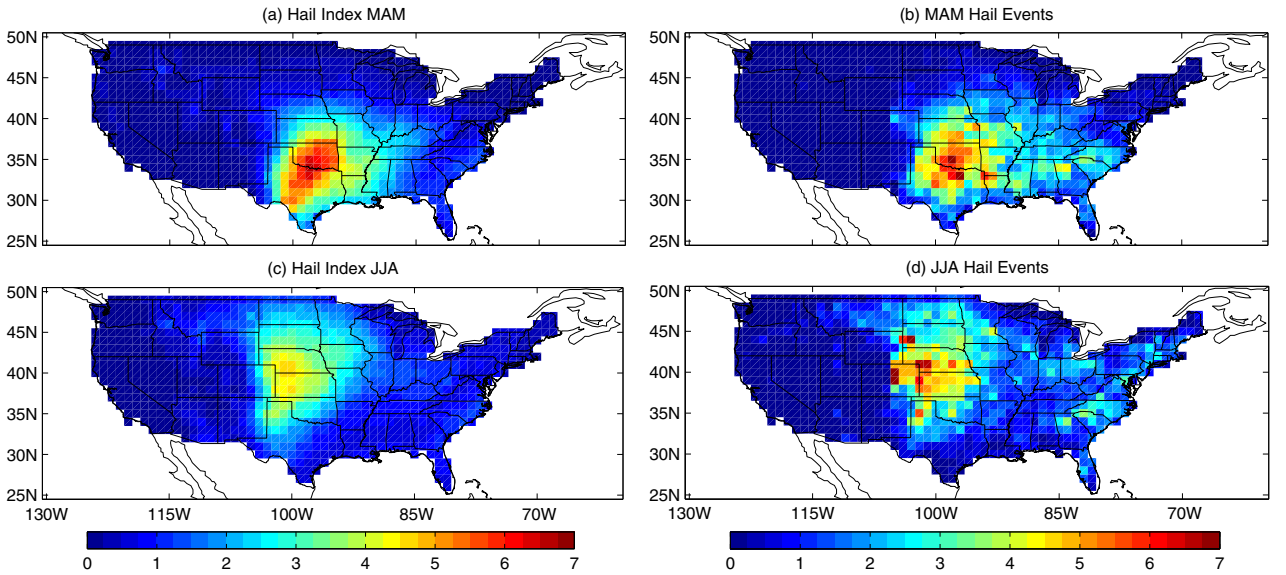

Figure 9. Seasonal mean number of three-hourly periods with large hail events from the four parameter index 1979–2012 for (a) March, April, May (MAM), (c) June, July, August (JJA), and observed three-hourly periods with large hail events over the same period for (b) MAM and (d) JJA.

related to the warning verification process, with hail climatologically less frequent in the area due to a reduced occurrence of high midlevel lapse rates and a predisposition to greater updraft moisture loading [*Cintineo et al*., 2012]. Additionally, a large part of the frequency, particularly further east, may reflect the occurrence of pulse-type thunderstorms during the summer months rather than the likelihood of organized storms that the model attempts to identify. These storms are primarily driven by thermodynamic and buoyancy processes rather than vertical wind shear, and are inherently difficult to forecast even on a diurnal timeframe.

Existing indices for large hail occurrence are difficult to compare to SSP and SHIP. These indices detect hail above 2 in., rather than 1 in. as in our hail model and use daily, not monthly data. SSP is also derived for all severe thunderstorm hazards and thus may include environments not favorable to large hail, while SHIP is calibrated for higher-resolution forecast model data. As a qualitative comparison, *Gensini and Ashley* [2011] produced a climatology of an SSP parameter from the NARR reanalysis for the period 1980–2009. The primary difference between our model and this climatology is the lower frequency (10 as compared to 20–30 environments per year) as well as the shift of the peak region westward and northward. The hail index also has reduced susceptibility to artificial inflation of favorable environments in southern Texas as described in section 3. Subjective testing of model performance against alternative climatology was also considered by calculating the mean annual frequency for the 2007–2010 period (not shown) used by *Cintineo et al*. [2012]. The distribution was found to be similar both in terms of peak frequency and spatial extent to the radar-derived climatology, although the peaks around radar observation areas were not replicated, and the model was biased eastward.

4.3. Seasonal Progression

A key test of the hail climatology is the handling of the progression of the seasonal cycle and its spatial variability. The spatial distributions of the climatology were divided into spring (MAM) and summer (JJA) periods (Figure 9). For MAM, the model performed similarly to the performance for the full year, with the relative RMSE of a similar value (Table 4). There is a slight bias toward the southeast, an overestimation near the Gulf coast and Mexican border, and deficiencies in frequency over the southeast (Figure 9b). The biases in southern Texas in the model, while improved relative to those identified using purely CAPE and shear parameters [e.g., *Brooks et al*., 2003; *Gensini and Ashley*, 2011], suggest that initiation remains a problem. The inclusion of cPrcp, a model-derived estimate of convective initiation produced by the model convective scheme, appears to be the source of much of this improvement, but given the known issues with

© 2015. The Authors.

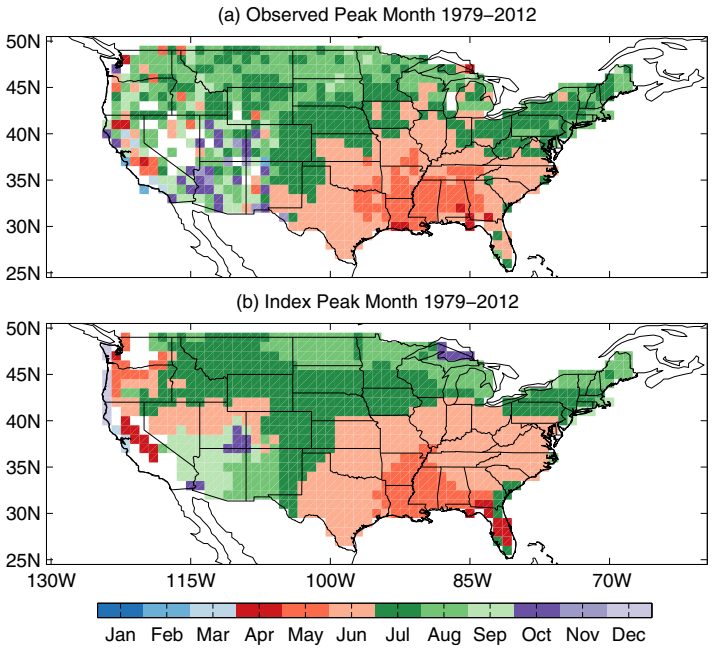

Figure 10. (a) Climatological mean peak month at each grid point of observed large hail events 1979–2012, and (b) climatological mean peak month at each grid point of the hail model 1979–2012.

convective parameterization schemes [e.g., *Allen et al*., 2014] it is unlikely to completely resolve the issue of whether a storm is possible in an environment or not.

During the summer months, the model correctly shifts the spatial distribution northwest, while decreasing the intensity (Figure 9c). In comparison to observations, there is a pronounced eastward bias resulting from moisture deficiencies closer to the Rockies, with lower frequency also found in the east (Figure 9d). The Colorado high plains, a region known to have some of the highest frequencies of hail occurrence [*Changnon et al*., 2009], is also problematic for the model. This deficiency likely arises from a low bias in moisture in the reanalysis as suggested by *Gensini et al*. [2014], and perhaps hail occurrence in environments where weaker SRH is offset by mesoscale influences [*Wakimoto and Wilson*, 1989].

Another way to evaluate the seasonal cycle in the model is to identify at each location the peak month of climatological frequency in the model and reports (Figure 10). Spatially, the peak month in reports shifts from the Gulf coast to the southern plains of Oklahoma in April and May, before shifting north and west during June and reaching the most northern margins of the continent by July. Overall, the model replicates well this northwest shift of peak month from the early spring in the southeast and to summer over the high plains. However, the model peaks later than observations in the west. The peak month in the northeast for the model also differs compared to observations, occurring in June rather than July, while the model also suggests a peak in Florida in the early spring when in observations this is found in the summer months. Remarkably, the model appears to identify the hail peak in the southwest over Arizona, associated with the tail end of the monsoon pattern (August–October) when moisture below 700 hPa is high and promotes severe thunderstorms [*Maddox et al*., 1995]. It is also noted that over the area west of the Rocky Mountains where few observations exist, the model pattern does not reproduce the sporadic observational peaks, despite the reported losses in this area [*Changnon et al*., 2009].

5. Interannual Variability and Trends

To this point, we have only evaluated the ability of the hail model to reproduce aspects of the annual cycle and seasonal distribution of the report climatology. We now test the ability of the hail model to capture interannual variability. We first use deviance as overall performance measure and use the hail model evaluated on climatological environment as a baseline. Figure 11 shows that the deviance of the hail model applied to interannually varying monthly environmental parameters is about 90% of the baseline. Replacing one of the parameters in the baseline by its interannually varying values is seen to have positive impact (deviance is reduced) for all of the parameters except Q_{mean}, indicating that all the parameters except Q_{mean} have predictive skill on independent data; interannually varying values of Q_{mean} increase the deviance of the hail model by about 5% with respect to the baseline.

To further evaluate the hail model on interannually varying data, we compute the correlation between the CONUS total number of hail events reported and predicted by the hail model for each calendar month

© 2015. The Authors.

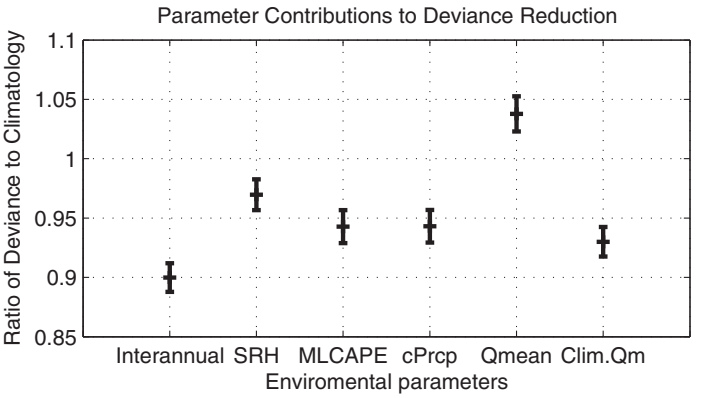

Figure 11. Contribution of the respective parameters to index deviance measured as a ratio of deviance using the interannually varying parameter to the climatological value, with spread from the standard deviation of deviance from cross-validated fitting. The value labeled Clim. Qm indicates the use of interannually varying values for all variables except Q_{mean}.

(Table 5). The correlation of the baseline model is zero for all months because it has no interannual variability. Again, we replace one of the parameters in the baseline by its interannually varying values to get an idea of the individual contributions of the environmental variables. The greatest portion of variability in the model can be explained by MLCAPE from November to April, with cPrcp also contributing during both December and January. As the season approaches the transitional period of spring, SRH plays a greater role for April through June, where instability is more commonly available, but strong rotational potential for storms overlapping instability is less common. In comparison to the other parameters, Q_{mean} shows poor correlations for the interannual data for much of the winter and spring.

The correlations between the number of hail events in each of the nine NOAA climate regions [*Karl and Koss*, 1984] and that predicted by the model show good skill (Table 3). The strongest interannual performance is found during the early season (January–May) for each of the south, southeast, central, upper midwest, plains, and northeast. These reflect the predominant conditions for producing large hail, involving storm initiation, instability, and wind shear that produce the hail peak frequency of the Great Plains and eastward along the progression of the Rocky mountain leeward extratropical cyclone track. The poorest performance is found over the southeast during the summer months corresponding to the buoyancy-driven processes over that region, and to a lesser extent over the northern plains when initiation becomes less predictable within reanalysis products. The reduced correlations over the summer months suggest that the index performance may be related to the annual cycle of synoptic-scale forcing. In some respects, this is unsurprising, as the index in the fitting procedure is weighted by the observations to represent the most frequent conditions producing large hail, and reflects the potential value of more adaptive fitting approaches. We note that while significant, correlations are significantly reduced by the changes in reporting over time and space, and thus it is unsurprising that correlations to the more recent period are considerably higher for many regions (not shown).

Artificial trends in observations are a considerable problem in the reported hail climatology as in the tornado climatology [*Doswell et al*., 2005; *Verbout et al*., 2006; *Brooks and Dotzek*, 2007]. Despite this, recent work using normalized insurance losses and environmental data has suggested increases to both frequency and variability of severe thunderstorm losses due to changes in the most extreme environments over the period 1970–2009 [*Sander et al*., 2013]. Increased variability and clustering of tornado reports and environments has also been reported [*Tippett*, 2014, *Brooks et al*., 2014]. Examining hail events, a strong positive trend is found in the total annual CONUS occurrence (Figure 12), which is similar to other observed trends in large hail and hail greater than 3 in. [*Doswell et al*., 2005; *Brooks and Dotzek*, 2007]. The evidence for the

Table 3. Pearson Correlations Between the Index and Reported Number of Hail Events Greater Than 1 n. With All Parameters Climatological Except the Listed Which Is Allowed to Interannually Vary[a]

	January	February	March	April	May	June	July	August	September	October	November	December	Annual
Four parameter	**0.85**	**0.66**	**0.61**	**0.66**	**0.44**	**0.42**	−0.10	−0.10	−0.03	0.32	**0.63**	**0.44**	0.22
SRH	0.19	0.04	0.07	**0.42**	**0.47**	**0.39**	**0.35**	0.29	0.01	0.02	**0.35**	0.22	**0.47**
MLCAPE	**0.82**	**0.60**	**0.72**	**0.52**	**0.46**	0.05	−0.19	**−0.42**	−0.15	**0.39**	**0.57**	**0.39**	0.16
cPrcp	**0.76**	0.31	0.34	**0.37**	−0.33	0.04	−0.14	−0.17	−0.01	0.10	0.28	**0.50**	−0.29
Q_{mean}	**−0.40**	**−0.42**	**−0.42**	**−0.39**	−0.12	0.12	0.21	0.36	0.20	0.00	0.01	−0.05	0.13

[a]Significant correlations determined via a *t* test are in bold.

© 2015. The Authors.

Table 4. Pearson Correlations Between the Index and Reported Number of Hail Events Greater Than 1 in. by U.S. Climate Region and Month for the Period 1979–2012[a]

	January	February	March	April	May	June	July	August	September	October	November	December	Annual
South	**0.81**	**0.77**	**0.44**	**0.65**	**0.41**	**0.54**	**0.59**	**0.47**	**0.39**	**0.36**	**0.69**	**0.43**	**0.35**
Southeast	**0.61**	0.29	**0.52**	**0.54**	**0.40**	0.07	0.03	0.32	0.00	0.05	**0.51**	**0.36**	0.11
Central	**0.77**	**0.51**	**0.81**	**0.72**	**0.72**	**0.76**	0.24	0.22	0.30	**0.43**	**0.36**	0.34	**0.70**
Upper MW	**0.59**	**0.42**	**0.79**	**0.51**	**0.81**	**0.48**	0.33	0.06	0.31	**0.48**	**0.50**	0.00	**0.38**
Plains	0.05	**0.43**	**0.65**	**0.55**	**0.58**	**0.42**	0.25	0.22	**0.35**	**0.63**	0.29	0.02	0.06
Northeast	**0.61**	**0.37**	**0.48**	**0.79**	**0.71**	**0.63**	**0.35**	**0.34**	**0.57**	0.16	**0.48**	0.21	**0.70**
Southwest	0.13	0.15	0.23	0.00	0.03	0.05	−0.20	−0.02	−0.04	**0.46**	0.31		**−0.48**
Northwest		−0.05	0.07	**0.35**	**0.40**	0.08	**0.38**	0.04	**0.41**	**0.40**			0.05
West	0.32	0.06	−0.16	**0.58**	0.26	**0.45**	0.08	0.17	0.18	**0.44**	0.10	−0.03	−0.06

[a]Significant correlations determined via a *t* test are in bold font. Regions and months with less than 34 years with reported hail events during the period are omitted.

Texas panhandle (Figure 2) suggests that this trend is not solely related to population, but may also be related to the influence of storm chasers and increasing portable telecommunications to simplify reporting procedures [*Tuovinen et al*., 2009]. The large influence of these nonphysical changes may therefore mask a trend in favorable environmental characteristics. Contrasting the trend in reports, changes in modeled hail events are negligible, which is consistent with the lack of trends found in prior analyses using mean environments or SSP over the CONUS domain with NARR and NCEP-NCAR reanalysis data [*Brooks and Dotzek*, 2007; *Kunz et al*., 2009; *Gensini and Ashley*, 2011; *Robinson et al*., 2013]. This does not imply that regional trends in environmental conditions are not present or only affect extreme values in the distribution [*Sander et al*., 2013]. However, using the modeled frequency of large hail over the CONUS there is no appreciable trend, which may either be related to the lack of a trend in the NARR reanalysis, or trends of opposite signal over smaller geographic regions.

To reduce the trend in CONUS observed reports, we apply a correction similar to the inflation adjustment applied to tornado observations (details of this adjustment can be found at http://www.spc.noaa.gov/wcm/adj.html) [*Tippett et al*., 2012]. Observed large hail events are linearly detrended to compare to the model annual totals, producing the adjusted observations. Absolute values need be carefully considered when analyzing detrended observations; however, the most noticeable features are the relative trough that occurs in the late 1980s, values that the observed frequency does not go below until 2007 and 2010. This is in contrast to the relative peaks that occur in both 2008 and 2011. These variations in frequency are qualitatively similar to those observed for the U.S. tornado record [*Tippett*, 2014], suggesting that detrended large hail is another potential proxy for supercells in historical climatology. Correlations in annual total between the observations and the model increase from 0.22 for the raw observational data to 0.57 for the detrended data. Compared to the adjusted frequency, variability in annual total appears to be well captured by the model. Discrepancies between the model and observations in peak values may be related to the smoothing of the adjustment procedure or more localized environment characteristics leading to hail occurrence. While this adjustment is applicable to the CONUS total, the differences in remaining variance suggested that further analysis over smaller regions was warranted.

On a regional scale, large variations in the annual total number of hail events are also found. These trends are difficult to correct using simple detrending, with increases of 4–5 times the number of hail events and discontinuities (not shown). In comparison, the model based on environmental values produces relatively stationary mean annual total numbers of hail events for each region, with little to no trend in most regions, consistent with previous analyses for severe thunderstorms [*Gensini and Ashley*, 2011; *Robinson et al*., 2013]. However, small negative trends in the model are identified in the plains, southwest, and the northwest, suggesting potential environmental influences. The presence of such large trends in the hail events makes evaluation of the ability of the model to represent trends in hail occurrence difficult and highlights that caution must be taken when considering trends over large spatial areas, and when considering reports that are subject to nonmeteorological factors. This suggests

Table 5. Root Mean Squared Error and Pattern Congruence (Uncentered Pattern Correlation [*Wilks*, 2006]) for the Hail Model as Compared to Observed Large Hail Events for the Entire Calendar Year and the Respective Seasons

	Annual	DJF	MAM	JJA	SON
RMSE	1.27	0.22	0.76	0.88	0.35
Pattern conguuence	0.93	0.76	0.91	0.88	0.85

© 2015. The Authors.

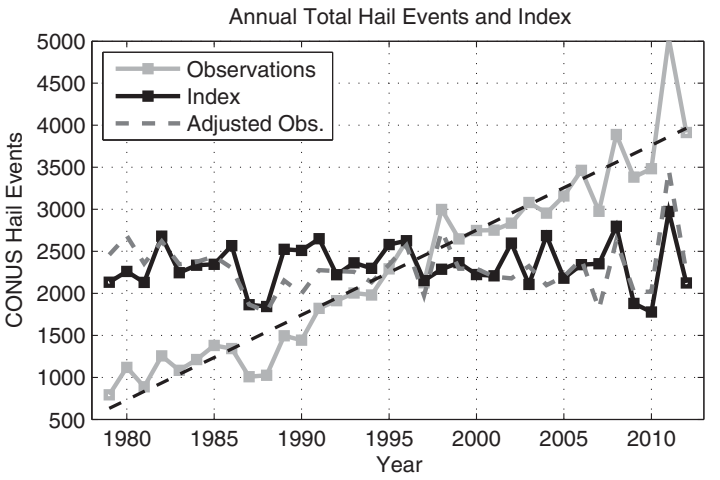

Figure 12. Variability in annual CONUS total of hail events as compared to the index for the period 1979–2012. Gray line shows occurrence of large hail events over the respective regions, while the black line shows the annual frequency as simulated by the four-parameter hail index. The adjusted observations (dashed gray) have been linearly detrended (trend shown in dashed black).

that alternative data sources, including other reanalyses, component ingredients, and remote observations, are necessary to understand whether such trends are artifacts of the data set or an actual climatic signal.

6. Conclusions

A new empirical model relating the monthly occurrence of large hail (greater than 1 in. in diameter) to monthly averaged, large-scale environment has been developed. Monthly hail occurrence is defined to be the number of three-hourly periods in a month that produce one or more reported occurrences of hail greater than 1 in. in a $1^\circ \times 1^\circ$ grid box. The model uses convective precipitation, storm relative helicity between the surface and 3 km, 180 hPa mixed-layer CAPE, and mean-specific humidity in the lowest 90 hPa of the atmosphere. The model differs in its choice of parameters and their weighting from existing indices for tornadoes [*Tippett et al*., 2012, 2014] and indices that were developed using multiple types of severe weather [*Brooks et al*., 2003; *Gensini and Ashley*, 2011; *Allen and Karoly*, 2014]. This model fits large hail whereas the indices developed using multiple types of severe thunderstorm hazards examined hail in excess of 2 in.

The model is developed in a regression framework using only climatological annual cycle data. The overall significance of the climatological relation between large hail events and monthly averaged environment is established through cross validation and significance testing. The model captures well the annual cycle of hail occurrence on both a continental and regional basis. The model also performs well in showing the spatial shifts of the climatological distribution of large hail over the year, with some problems in simulating variability, particularly during the summer where underestimation occurs, and during fall where the modeled hailstone numbers do not decrease sufficiently. The representation of the seasonal cycle is best from the south to central plains and through the midwest. The model does not capture the westward shift in peak frequency early enough, which appears to be related to moisture biases in the NARR product.

Application of the model to interannually varying data provides a further test which is independent of the climatological data used to develop the model. All the environmental variables except Q_{mean} are shown to explain to interannual variability of hail occurrence on both a continental scale and regional basis. The annual mean frequency does not display the spatially variable changes seen in reports, confirming that these trends are not due to these environmental factors. Analyzing this frequency as a CONUS total further reinforces that there is no trend on a continent-wide basis in the index. Comparing to detrended observed hail data, the resulting inflation adjusted hail frequency is similar to that of the model.

A fundamental limitation of the model developed here is that monthly averaged environmental values are clearly removed from the diurnal variability of the component ingredients and parameters most directly connected to severe convection. However, this work has demonstrated that the extreme environments associated with large hail do have a significant expression in the monthly mean environment values. Of course, isolated events would not be expected to be well captured by monthly averages. Despite these limitations, the model appears to agree well with ongoing projects to supplement the observational data using remote sensing sources such as radar [*Cintineo et al*., 2012, Figures 9 and 11] and provides a useful tool for relating severe weather to climate variability and estimating the influence of potential changes to the climate.

© 2015. The Authors.

Acknowledgments
The authors are supported by grants from the National Oceanic and Atmospheric Administration (NA05OAR4311004 and NA14OAR4310185), the Office of Naval Research (N00014-12-1–0911), and a Columbia University Research Initiatives for Science and Engineering (RISE) award. The views expressed herein are those of the authors and do not necessarily reflect the views of NOAA or any of its subagencies. Data for the observations used in this study were sourced from the NCDC Storm Events database for hail available at http://www.ncdc.noaa.gov/stormevents/ftp.jsp, while North American Regional Reanalysis data used to produce the hail environment index are available at http://nomads.ncdc.noaa.gov/data.php?name=access#narr_datasets.

References

Allen, J. T., and D. J. Karoly (2014), A climatology of Australian severe thunderstorm environments 1979–2011: Inter-annual variability and ENSO influence, *Int. J. Climatol.*, *34*, 81–97.

Allen, J. T., D. J. Karoly, and K. J. Walsh (2014), Future Australian severe thunderstorm environments. Part I: A novel evaluation and climatology of convective parameters from two climate models for the late twentieth century, *J. Clim.*, *27*, 3827–3847.

Baldwin, M. E., J. S. Kain, and M. P. Kay (2002), Properties of the convection scheme in NCEP's Eta Model that affect forecast sounding interpretation, *Weather Forecasting*, *17*, 1063–1079.

Blair, S., D. E. Cavanaugh, J. Laflin, J. Leighton, and K. Sanders (2014), High-resolution hail observations: Implications for NWS warning operations and climatological data, in *26th Conference on Weather Analysis and Forecasting, Atlanta, GA*, Am. Meteorol. Soc. AMS online, 18.1.

Brooks, H. E. (2009), Proximity soundings for severe convection for Europe and the United States from reanalysis data, *Atmos. Res.*, *93*, 546–553.

Brooks, H. E. (2013), Severe thunderstorms and climate change, *Atmos. Res.*, *123*, 129–138.

Brooks, H. E., and N. Dotzek (2007), The spatial distribution of severe convective storms and an analysis of their secular changes, in *Climate Extremes and Society*, edited by Henry F. Diaz and Richard J. Murnane, pp. 35–54, Cambridge University Press, N. Y. [Available at: http://www.cambridge.org/US/academic/subjects/earth-and-environmental-science/climatology-and-climate-change/climate-extremes-and-society.]

Brooks, H. E., J. W. Lee, and J. P. Craven (2003), The spatial distribution of severe thunderstorm and tornado environments from global reanalysis data, *Atmos. Res.*, *67*, 73–94.

Brooks, H. E., G. W. Carbin, and P. T. Marsh (2014), Increased variability of tornado occurrence in the United States, *Science*, *346*, 349–352.

Bukovsky, M. S., and D. J. Karoly (2007), A brief evaluation of precipitation from the North American regional reanalysis, *J. Hydrometeorol.*, *8*, 837–846.

Cao, Z. (2008), Severe hail frequency over Ontario, Canada: Recent trend and variability, *Geophys. Res. Lett.*, *35*, L14803, doi:10.1029/2008GL034888.

Cecil, D. J., and C. B. Blankenship (2012), Toward a global climatology of severe hailstorms as estimated by satellite passive microwave imagers, *J. Clim.*, *25*, 687–703.

Changnon, S. A. (1999), Data and approaches for determining hail risk in the contiguous United States, *J. Appl. Meteorol.*, *38*, 1730–1739.

Changnon, S. A. (2008), Temporal and spatial distributions of damaging hail in the continental United States, *Phys. Geogr.*, *29*, 341–350. Urbana-Champaign, Ill.

Changnon, S. A., D. Chagnon, and S. D. Hilberg (2009), Hailstorms across the nation: An atlas about hail and its damages, *Contract Rep. 2009-12*, 95 pp., State Water Surv., Ill.

Cintineo, J. L., T. M. Smith, V. Lakshmanan, H. E. Brooks, and K. L. Ortega (2012), An objective high-resolution hail climatology of the contiguous United States, *Weather Forecasting*, *27*, 1235–1248.

Craven, J. P., R. E. Jewell, and H. E. Brooks (2002), Comparison between observed convective cloud-base heights and lifting condensation level for two different lifted parcels, *Weather Forecasting*, *17*, 885–890.

Davis, S. M., and J. LaDue (2004), Nonmeteorological factors in warning verification, in *22nd Conference on Severe Local Storms*, *Hyannis, MA*,, vol. 7, 4 pp., Am. Meteorol. Soc.

Doswell, C. A. (2007), Small sample size and data quality issues illustrated using tornado occurrence data, *Electron. J. Severe Storms Meteorol.*, *2*, 1–16.

Doswell, C. A., and P. M. Markowski (2004), Is buoyancy a relative quantity?, *Mon. Weather Rev.*, *132*, 853–863.

Doswell, C. A., H. E. Brooks, and M. P. Kay (2005), Climatological estimates of daily local nontornadic severe thunderstorm probability for the United States, *Weather Forecasting*, *20*, 577–595.

Eccel, E., P. Cau, K. Riemann-Campe, and F. Biasioli (2012), Quantitative hail monitoring in an alpine area: 35-year climatology and links with atmospheric variables, *Int. J. Climatol.*, *32*, 503–517.

Edwards, R., and R. L. Thompson (1998), Nationwide comparisons of hail size with WSR-88D vertically integrated liquid water and derived thermodynamic sounding data, *Weather Forecasting*, *13*, 277–285.

Elsner, J. B., and H. M. Widen (2014), Predicting spring tornado activity in the central Great Plains by 1 March, *Mon. Weather Rev.*, *142*, 259–267.

Gensini, V. A., and W. S. Ashley (2011), Climatology of potentially severe convective environments from the North American regional reanalysis, *Electron. J. Severe Storms Meteorol.*, *6*, 1–40.

Gensini, V. A., T. L. Mote, and H. E. Brooks (2014), Severe thunderstorm reanalysis environments and collocated radiosonde observations, *J. Appl. Meteorol. Climatol.*, *53*, 742–751, doi:10.1175/JAMC-D-13-0263.1.

Giaiotti, D., S. Nordio, and F. Stel (2003), The climatology of hail in the plain of Friuli Venezia Giulia, *Atmos. Res.*, *67–68*, 247–259.

Grams, J. S., R. L. Thompson, D. V. Snively, J. A. Prentice, G. M. Hodges, and L. J. Reames (2012), A climatology and comparison of parameters for significant tornado events in the United States, *Weather Forecasting*, *27*, 106–123.

Groenemeijer, P., and A. Van Delden (2007), Sounding-derived parameters associated with large hail and tornadoes in the Netherlands, *Atmos. Res.*, *83*, 473–487.

Hales, J. E., Jr. (1993), Biases in the severe thunderstorm data base: Ramifications and solutions, in *13th Conference on Weather Forecasting and Analysis, Vienna, VA*, pp. 504–507, Am. Meteorol. Soc.

Jewell, R., and J. Brimelow (2009), Evaluation of Alberta hail growth model using severe hail proximity soundings from the United States, *Weather Forecasting*, *24*, 1592–1609.

Kapsch, M.-L., M. Kunz, R. Vitolo, and T. Economou (2012), Long-term trends of hail-related weather types in an ensemble of regional climate models using a Bayesian approach, *J. Geophys. Res.*, *117*, D15107, doi:10.1029/2011JD017185.

Karl, T. R., and W. J. Koss (1984), Regional and National Monthly, Seasonal, and Annual Temperature Weighted by Area, 1895–1983, Hist. Climatol. Ser., vol. 4, 38 pp., Natl. Clim. Data Cent., Asheville, N. C.

Kelly, D. L., J. T. Schaefer, and C. A. Doswell III (1985), Climatology of nontornadic severe thunderstorm events in the United States, *Mon. Weather Rev.*, *113*, 1997–2014.

Knight, C. A., and N. C. Knight (2001), Hailstorms, in *Severe Convective Storms*, *Meteorol. Monogr.*, edited by Charles A. Doswell, Am. Meteorol. Soc., vol. 28, pp. 223–248, Boston, Mass.

Kunz, M., J. Sander, and C. Kottmeiera (2009), Recent trends of thunderstorm and hailstorm frequency and their relation to atmospheric characteristics in southwest Germany, *Int. J. Climatol.*, *29*, 2283–2297, doi:10.1002/joc.1865.

© 2015. The Authors.

Maddox, R. A., D. M. McCollum, and K. W. Howard (1995), Large-scale patterns associated with severe summertime thunderstorms over central Arizona, *Weather Forecasting*, *10*, 763–778.
Manzato, A. (2012), Hail in northeast Italy: Climatology and bivariate analysis with the sounding-derived indices, *J. Appl. Meteorol. Climatol.*, *51*, 449–467.
Manzato, A. (2013), Hail in northeast Italy: A neural network ensemble forecast using sounding-derived indices, *Weather Forecasting*, *28*, 3–28, doi:10.1175/WAF-D-12-00034.1.
Mesinger, F., et al. (2006), North American regional reanalysis, *Bull. Am. Meteorol. Soc.*, *87*, 343–360
Munich, R. E. (2013), Severe weather in North America, report, 302-07563, 274 pp., Munich, Germany.
Ortega, L., T. M. Smith, K. L. Manross, K. A. Scharfenberg, A. Witt, A. G. Kolodziej, and J. J. Gourley (2009), The severe hazards analysis and verification experiment, *Bull. Am. Meteorol. Soc.*, *90*, 1519–1530.
Robinson, E. D., R. J. Trapp, and M. E. Baldwin (2013), The geospatial and temporal distributions of severe thunderstorms from high-resolution dynamical downscaling, *J. Appl. Meteorol. Climatol.*, *52*, 2147–2161, doi:10.1175/JAMC-D-12-0131.1.
Sander, J., J. F. Eichner, E. Faust, and M. Steuer (2013), Rising variability in thunderstorm-related U.S. losses as a reflection of changes in large-scale thunderstorm forcing, *Weather Clim. Soc.*, *5*, 317–331, doi:10.1175/WCAS-D-12-00023.1.
Sanderson, M., W. Hand, P. Groenemeijer, P. Boorman, J. Webb, and L. McColl (2014), Projected changes in hailstorms during the 21st century over the UK, *Int. J. Climatol.*, *35*, 15–24, doi:10.1002/joc.3958.
Schaefer, J. T., and R. Edwards (1999), The SPC tornado/severe thunderstorm database, in *11th Conference on Applied Climatology*, pp. 215–220, Am. Meteorol. Soc., Dallas, Tex.
Schaefer, J. T., J. J. Levit, S. J. Weiss, and D. W. McCarthy (2004), The frequency of large hail over the contiguous United States, in *14th Conference on Applied Climatology*, *Seattle, WA*, 7 pp., Am. Meteorol. Soc., CD-ROM, P7.8.
Stumpf, G. J., T. Smith, and J. Hocker (2004), New hail diagnostic parameters derived by integrating multiple radars and multiple sensors, in *22nd Conference on Severe Local Storms*, *Hyannis, MA*, *Am. Meteorol. Soc.*
Thompson, R. L., B. T. Smith, J. S. Grams, A. R. Dean, and C. Broyles (2012), Convective modes for significant severe thunderstorms in the contiguous United States. Part II: Supercell and QLCS tornado environments, *Weather Forecasting*, *27*, 1136–1154.
Tippett, M. K. (2014), Changing volatility of US annual tornado reports, *Geophys. Res. Lett.*, *41*, 6956–6961, doi:10.1002/2014GL061347.
Tippett, M. K., S. J. Camargo, and A. H. Sobel (2011), A Poisson regression index for tropical cyclone genesis and the role of large-scale vorticity in genesis, *J. Clim.*, *24*, 2335–2357.
Tippett, M. K., A. H. Sobel, and S. J. Camargo (2012), Association of U.S. tornado occurrence with monthly environmental parameters, *Geophys. Res. Lett.*, *39*, L02801, doi:10.1029/2011GL050368.
Tippett, M. K., A. H. Sobel, S. J. Camargo, and J. T. Allen (2014), An empirical relation between U.S. tornado activity and monthly environmental parameters, *J. Clim.*, *27*, 2983–2999, doi:10.1175/JCLI-D-13-00345.1.
Trapp, R. J., D. M. Wheatley, N. T. Atkins, R. W. Przybylinski, and R. Wolf (2006), Buyer beware: Some words of caution on the use of severe wind reports in postevent assessment and research, *Weather Forecasting*, *21*, 408–415.
Trapp, R. J., N. S. Diffenbaugh, and A. Gluhovsky (2009), Transient response of severe thunderstorm forcing to elevated greenhouse gas concentrations, *Geophys. Res. Lett.*, *36*, L01703, doi:10.1029/2008GL036203.
Tuovinen, J.-P., A.-J. Punkka, J. Rauhala, H. Hohti, and D. M. Schultz (2009), Climatology of severe hail in Finland: 1930–2006, *Mon. Weather Rev.*, *137*, 2238–2249, doi:10.1175/2008MWR2707.1.
Verbout, S. M., H. E. Brooks, L. M. Leslie, and D. M. Schultz (2006), Evolution of the U.S. tornado database: 1954–2003, *Weather Forecasting*, *21*, 86–93.
Wakimoto, R. M., and J. W. Wilson (1989), Non-supercell tornadoes, *Mon. Weather Rev.*, *117*, 1113–1140, doi:10.1175/1520-0493(1989)117%1113:NST%2.0.CO;2.
Wilks, D. S. (2006), *Statistical Methods in the Atmospheric Sciences*, vol. 59, 627 pp., Academic Press, Elsevier, Burlington, Mass.
Wyatt, A., and A. Witt (1997), The effect of population density on ground-truth verification of reports used to score a hail detection algorithm, in *28th Conference on Radar Meteorology*, *Austin, TX*, pp. 368–369, Am. Meteorol. Soc.

© 2015. The Authors.